

# Identification of mouse crystallins in 2D protein patterns by sequencing and mass spectrometry. Application to cataract mutants

P.R. Jungblut<sup>a</sup>, A. Otto<sup>b</sup>, J. Favor<sup>c</sup>, M. Löwe<sup>d</sup>, E.-C. Müller<sup>b</sup>, M. Kastner<sup>e</sup>, K. Sperling<sup>d</sup>, J. Klose<sup>d,\*</sup>

<sup>a</sup>Max-Planck-Institut für Infektionsbiologie, Proteinanalytik, D-10117 Berlin, Germany

<sup>b</sup>Max-Delbrück-Center für Molekulare Medizin, Proteinchemie, D-13125 Berlin, Germany

<sup>c</sup>GSF-Forschungszentrum Neuherberg, Institut für Säugetiergenetik, D-85758 Oberschleißheim, Germany

<sup>d</sup>Humboldt-Universität, Charité, Virchow-Klinikum, Institut für Humangenetik, Augustenburger Platz 1, D-13353 Berlin, Germany

<sup>e</sup>Freie Universität Berlin, Benjamin Franklin Klinikum, Institut für Klinische Pharmakologie, D-14195 Berlin, Germany

Received 16 June 1998; revised version received 14 August 1998

**Abstract** The eye lens proteins of the mouse were separated into 1940 polypeptide spots by two-dimensional electrophoresis in large gels. All 16 crystallins ubiquitous in mammals were identified by protein sequencing and mass spectrometry except for ( $\gamma$ )-F, which shows an almost identical sequence with ( $\gamma$ )-E. Two crystallins, ( $\beta$ )-A2 and ( $\gamma$ )-S, were shown for the first time to occur in the mouse lens. An investigation of the murine cataract mutant *Cat2<sup>uop</sup>* (( $\gamma$ )-B gene) demonstrated that a monogenic mutation might affect a broad spectrum of proteins.

© 1998 Federation of European Biochemical Societies.

**Key words:** Mouse; Eye lens; Crystallin; Cataract; Two-dimensional electrophoresis; Mass spectrometry

## 1. Introduction

The eye lens can be regarded as a protein container organized in many concentric protein layers, which develop constantly from embryonic stage E11 throughout life [1]. The vast majority of these proteins, i.e. 80–90%, belong to one particular protein family, the crystallins. The sequence, structure and quantity of the individual crystallins determine the intermolecular interactions of these proteins and consequently the supramolecular organization of the lens. The short-range, glass-like order of the crystallins accounts for eye lens transparency [2]. Phase changes in the supramolecular structure of the lens can lead to opacity. Therefore, mutations in crystallin genes affecting the structure or amount of a certain crystallin or its spatial or temporal occurrence can result in eye lens defects such as cataracts.

In the mouse about 170 independent cataract mutations have been induced chemically or by radiation and characterized phenotypically ([3,4]; Favor, unpublished). Mouse lines were raised from these mutants and used for allelism studies [5], gene mapping and sequencing [6–9] and investigations on gene expression [10–12] in order to characterize mutations responsible for cataract development. To understand the etiology and pathogenesis of genetic lens defects the detection and identification of the individual crystallins (and other lens proteins) including information on their post-translational

modifications, their relative amounts and changes during development and aging are essential.

The crystallins occurring in all mammalian species were classified into crystallin ( $\alpha$ )-A and ( $\alpha$ )-B, ( $\beta$ )-A1 through ( $\beta$ )-A4 and ( $\beta$ )-B1 through ( $\beta$ )-B3, ( $\gamma$ )-A through ( $\gamma$ )-F and ( $\gamma$ )-S. In addition, several taxon-specific crystallins are known [1]. All common human crystallins have been sequenced and identified in two-dimensional (2D) electrophoresis patterns [13–17]; the ( $\beta$ )-A2, ( $\gamma$ )-E and F, however, do not occur in the human lens [17]. In mouse and rat the crystallin family has not been analyzed completely. 2D electrophoresis patterns of mouse lens proteins were used for detecting changes in the level of different crystallins in *CatFraser* mouse mutants [18], in buthionine sulfoximine treated mice [19], and in transgenic mice [20].

In the investigation presented here we resolved the total lens proteins of the mouse by large gel 2D electrophoresis, a high performance 2D technique leading to maximum resolution [21]. In the resulting protein pattern we identified by Edman degradation and mass spectrometry (MS) all the common crystallins except ( $\gamma$ )-F, which shows more than 95% sequence similarity to crystallin ( $\gamma$ )-E. By analyzing the murine cataract mutant *Nop*, we demonstrate that highly resolved, well-standardized and informative 2D electrophoresis patterns of mouse lens proteins can be used to study the effect of gene mutations on individual crystallins.

## 2. Materials and methods

### 2.1. Mouse strains

The mice investigated were from the Institut für Säugetiergenetik, GSF-Forschungszentrum Neuherberg and originated from mouse strains used in this institute for detecting induced mutations by the specific locus test [22]. Normal eye lenses were taken from (102/E1×C3H/E1) F<sub>1</sub> mice (five females, five males, 33–51 weeks old), cataract mutants (two males, 42 weeks) from strain 359 bearing the mutation *Nop* (allele symbol *Cat2<sup>uop</sup>*). Mutation 359 is of spontaneous origin [10] and has been shown to be a frameshift mutation (*Crygb<sup>uop</sup>*) of the *Crygb* gene, the gene of the ( $\gamma$ )-B crystallin [9].

### 2.2. Extraction of lens proteins

Mouse lenses were dissected from the eyes leaving the lens capsule intact. The two lenses of an individual were rinsed with physiological saline, freed from any adjacent fluid, weighed and frozen immediately in liquid nitrogen. A mortar and pestle were pre-cooled in liquid nitrogen. The following components were added to the mortar and were ground down to a fine powder: a pair of lenses (*a* mg; e.g. 13.7 mg), buffer (*a* mg×8 = *b*  $\mu$ l), protease inhibitor 1 (*[a* mg + *b*  $\mu$ l]×0.08 = *c*  $\mu$ l), protease inhibitor 2 (*[a* mg + *b*  $\mu$ l]×0.02 = *d*  $\mu$ l). Buffer: phosphate buffer pH 7.1 containing 0.2 M KCl, 5.1% CHAPS (= 4.5% in the final homogenate), 20% glycerol. Inhibitor 1: one cock-

\*Corresponding author. Fax: (49) (30) 450 66904.

E-mail: [klose@ukrv.de](mailto:klose@ukrv.de)

**Abbreviations:** 2D, two-dimensional; MS, mass spectrometry

Table 1  
 Mouse crystallins identified in 2D electrophoresis patterns of eye lens proteins by Edman degradation, PSD-MALDI-MS and peptide mass fingerprinting

Crystallins ubiquitous in mammalian eye lens	Analysis of proteins from 2D gels			Matching protein species from database		
	Spot No.	Sequence of peptide <sup>a</sup>	Peptide mass	Species	Identification No. <sup>b</sup>	Residue No.
(α)-A	25	QSLFR TVLDSEIGSEVRC		mouse	CRAA_RAT (SP)	50–54 55–65
(α)-A	182	ALGPFYPSR	1007	mouse	CRAA_RAT (SP) CRA2_MOUSE (SP)	13–21
(α)-B	176	APSWIDTGL FSVNLDV VLGDVIEVH IPADVDP EEKPAVAAAPC		mouse	CRAB_MOUSE (SP)	57–65 75–81 93–101 124–131 164–173
(β)-A1	280	ITIIDQENFQ GK NFDNVR ITNF EK		mouse	CRBA_MOUSE (SP)	16–27 42–47 109–114
(β)-A1	29	ITIFDQENFQ G NFDNV GEYP SYLSR		mouse	CRBA_MOUSE (SP)	16–26 42–46 74–77 –
(β)-A2	158	TYSDFGTQAHTGQLQSIR	2010	bovine	CRBB_BOVIN (SP)	175–192
(β)-A3	423	ELETLPPTTKC		human	CRBA_HUMAN (SP)	9–17
(β)-A4	35	MVVWDEEGFQGY		bovine	CRBD_BOVIN (SP)	27–38
(β)-B1	57	GEMFVLC	1036 (Mox)	rat	CRB1_RAT (SP)	107–113
(β)-B2	115	WDSWTSSRC TDSLSSLRPIKC	1024 1216 1409 2076	mouse	CRB2_MOUSE (SP)	81–88 90–99 108–119 48–67
(β)-B3	167	QYVFERC VINGTWVGYEFPGYRC		rat	CRB3_RAT (SP)	170–175 153–167
(β)-B3	226	VASIR QYVFERC VINGTXVGYC GEQFVLEKC		rat	CRB3_RAT (SP)	148–152 170–175 153–165 76–83
(γ)-A	247	ITFYEDR GFQGR GDYDPYQQWGMGFX QYLLRPGDYRC	944 1281 1049 2113 (Wox, Mox) 2788	mouse	CRGA_MOUSE (SP)	3–9 10–14 60–71 142–151 80–88 60–76 37–58 4–9
(γ)-B	223	ITFFED VDSGCWML GEYDPYQQXMGFSDS GQMSEITDC YLDWGAANAKC		mouse	S33523 (PIR)	38–45 61–75 101–108 155–164
(γ)-B	224	ITFFEDR LIPQHSPTYR YLDWGAANAKC DDFR	1171 1112 (kynurenine)	mouse	S33523 (PIR)	4–10 81–90 155–164 97–100
(γ)-C	239	IXFFEDR QYLLRPQEYR FQDWGSVDAK VVDLY FQDWGSVDAKC	928 1365 1184 (Wox) – 2125 2281 1155 (kynurenine)	mouse	S33526 (PIR) CRGC_MOUSE (SP)	4–10 143–152 154–163 170–174 61–77 60–77 154–163

(continued on next page)

tail tablet Complete (Boehringer Mannheim, Mannheim, Germany) dissolved in 2 ml buffer. Inhibitor 2: a mixture of one part pepstatin A (9.6 mg in 100 ml ethanol, dissolved at 37°C) and one part phenylmethylsulfonyl fluoride (1.742 g in 100 ml ethanol). The powder was transferred into a 1.5 ml Eppendorf tube, then thawed and sonicated in an ice cold water bath, six times for 10 s with intervals of 110 s. Glass beads, 2.2–2.5 mm in diameter, were added to the homogenate for sonication ( $[a \text{ mg} + b \mu\text{l} + c \mu\text{l} + d \mu\text{l}] \times 0.034 = \text{number of glass beads}$ ). After sonication and removal of the beads, the homogenate

was weighed ( $e \text{ mg}$ ) and stirred for 30 min in the cold room. The homogenate was mixed with urea ( $e \text{ mg} \times 1.08$ ) and 1.54 M DTT ( $e \text{ mg} \times 0.1$ ), stirred for 45 min at room temperature, and then mixed with ampholytes (Servalyte) pH 2–4 ( $e \text{ mg} \times 0.1$ ). The final concentrations of the additives were 9 M urea, 70 mM DTT, 2% ampholytes. The resulting sample was stored in aliquots at  $-70^\circ\text{C}$  and diluted with 1 part diluent (9 M urea, 70 mM DTT, 2% Servalyte pH 2–4 in bidistilled water) before analysis. For 2D electrophoresis 4  $\mu\text{l}$  of the sample was applied to a 44.5 cm IEF tube gel. Note that the proce-

Table 1 (continued)

Crystallins ubiquitous in mammalian eye lens	Analysis of proteins from 2D gels			Matching protein species from database		
	Spot No.	Sequence of peptide <sup>a</sup>	Peptide mass	Species	Identification No. <sup>b</sup>	Residue No.
(γ)-D	224	<b>QYLLRPGEYR</b>	942 1349 <sup>c</sup> 1396 (Wox, Mox) <sup>c</sup> 1835 <sup>c</sup> 846 (Mox) 1193 <sup>c</sup> 1256 <sup>c</sup>		CYMSG1 (PIR)	143–152
		<b>GDYDPY</b>				61–66
		<b>GFQGR</b>				11–15
		<b>S/PGEY</b>				148–151
		<b>VGSLR</b>				164–168
		<b>ITFYEDR</b>				4–10
		<b>ITFYEDR</b>				153–163
		<b>ITFYEDR</b>				153–163
		<b>ITFYEDR</b>				100–115
		<b>ITFYEDR</b>				169–174
(γ)-E	246	<b>ITFYEDR</b>	942 564 1295 1219 2098	mouse	CYMSG2 (PIR) JS0596 (PIR) S26811 (PIR)	4–10
		<b>GFQGR</b>				11–15
		<b>QYLLRPGEY</b>				143–152
		<b>YHDWGAMNAR<sup>c</sup></b>				154–163
		<b>YHDWGAMNAR<sup>c</sup></b>				61–77
(γ)-E	224	<b>QYLLRPGEYR</b>	1295 942 580 2098 (Wox, Mox) 942 1295	mouse	CYMSG2 (PIR) JS0596 (PIR) S26811 (PIR)	143–152
		<b>GDYDPY</b>				61–66
		<b>GFQGR</b>				11–15
		<b>S/PGEY</b>				148–151
		<b>VGSLR</b>				164–168
		<b>ITFYEDR</b>				4–10
		<b>ITFYEDR</b>				92–95
		<b>IYER<sup>c</sup></b>				61–77
		<b>ITFYEDR</b>				4–10
		<b>GDYDPYQQWMGF</b>				61–72
(γ)-E	232	<b>ITFYEDR</b>	942	mouse	CYMSG2 (PIR) JS0596 (PIR) S26811 (PIR)	4–10
		<b>IMDFY<sup>c</sup></b>				170–174
(γ)-F <sup>d</sup>			1295			143–152
(γ)-S	258	<b>ISFYEDR</b>	929 929 1888	bovine	CRBS_BOVIN (SP)	7–13
		<b>QYLL</b>				148–151
		<b>NFQGR<sup>c</sup></b>				14–18
		<b>VSEGTXIFYELPNY</b>				131–144

<sup>a</sup>Amino acids written in bold type are not in agreement with the sequence database.

<sup>b</sup>SP: SwissProt; PIR: Protein Identification Resource.

<sup>c</sup>Discriminative peptide.

<sup>d</sup>See text.

cedure described did not include a centrifugation step. A more detailed description of our highly standardized sample preparation procedure for 2D electrophoresis is given elsewhere [23].

### 2.3. 2D electrophoresis and image analysis

Two-dimensional electrophoresis was performed using the large gel technique described by Klose and Kobalz [21,24]. For separating lens proteins the ampholyte mixture was altered to spread the crystallin spots more in the horizontal direction (i.e. according to charge). The mixture consisted of one part Pharmalyte pH 3.5–10 and three parts Pharmalyte pH 5–8. From each of the 10 normal animals included in this investigation, a 2D pattern of total lens proteins was produced. One of these patterns was scanned with a laser scanner (type MD 300A, Molecular Dynamics, Krefeld, Germany), digitalized using a VAX station and transferred into a graphic spot pattern employing the spot detection program developed by Prehm et al. [25]. The pattern revealed by image analysis was corrected interactively on the terminal screen by comparison with the original gel pattern. The resulting pattern was checked visually against each of the nine other 2D patterns to ensure that each spot (except tiny spots at the detection limit) of the primary standard pattern was representative of mouse eye lens proteins. The final standard pattern was saved in the computer as a reference pattern for any information obtained for individual spots in further investigations.

### 2.4. Blotting

The proteins from 2D gels were blotted onto PVDF membranes as described [26] and stained with sulforhodamine [27]. For this purpose

2D electrophoresis was performed as indicated above with the exception that the sample was not diluted with one part diluent and 5 µl of the sample was applied to the IEF gel instead of 4 µl. Spots were cut from the membrane and collected from three runs. This gave sample material for the analytical studies.

### 2.5. Tryptic digestion and HPLC

Three cut spots per protein were incubated in 10–30 µl of 50 mM Tris-HCl, pH 7.8, 1 mM CaCl<sub>2</sub>, 10% v/v acetonitrile, 1% w/v octyl-β-D-glucopyranoside and 0.2–0.5 µg modified trypsin (Promega, Madison, WI, USA) for 15 h at 37°C. After incubation the extract was transferred to a 0.5 ml Eppendorf vial and the membrane pieces were washed first with 20–50 µl of 0.1% v/v trifluoroacetic acid (TFA) and then with 20–50 µl of 60% v/v acetonitrile/0.1% v/v TFA. Washing was supported by sonication. The membrane pieces were collected at the bottom of the tube by centrifugation. All supernatants were combined with the primary extract. After speed vac concentration 10% of the sample was used for peptide mass mapping and 90% was applied to micro-HPLC (Smart system, Pharmacia, Freiburg, Germany) in 0.1% v/v TFA at a flow rate of 100 µl/min. The peptides were eluted in a gradient of increasing acetonitrile concentrations, for more details see [28]. The peptide containing fractions were used for Edman degradation and MS.

### 2.6. Protein sequencing and MALDI-MS

Edman degradation of eluted peptides was performed in a Procise sequencer (Perkin Elmer, Weiterstadt, Germany). Peptide mass fingerprinting was performed in a time-of-flight VG TOF Spec (Fisons,

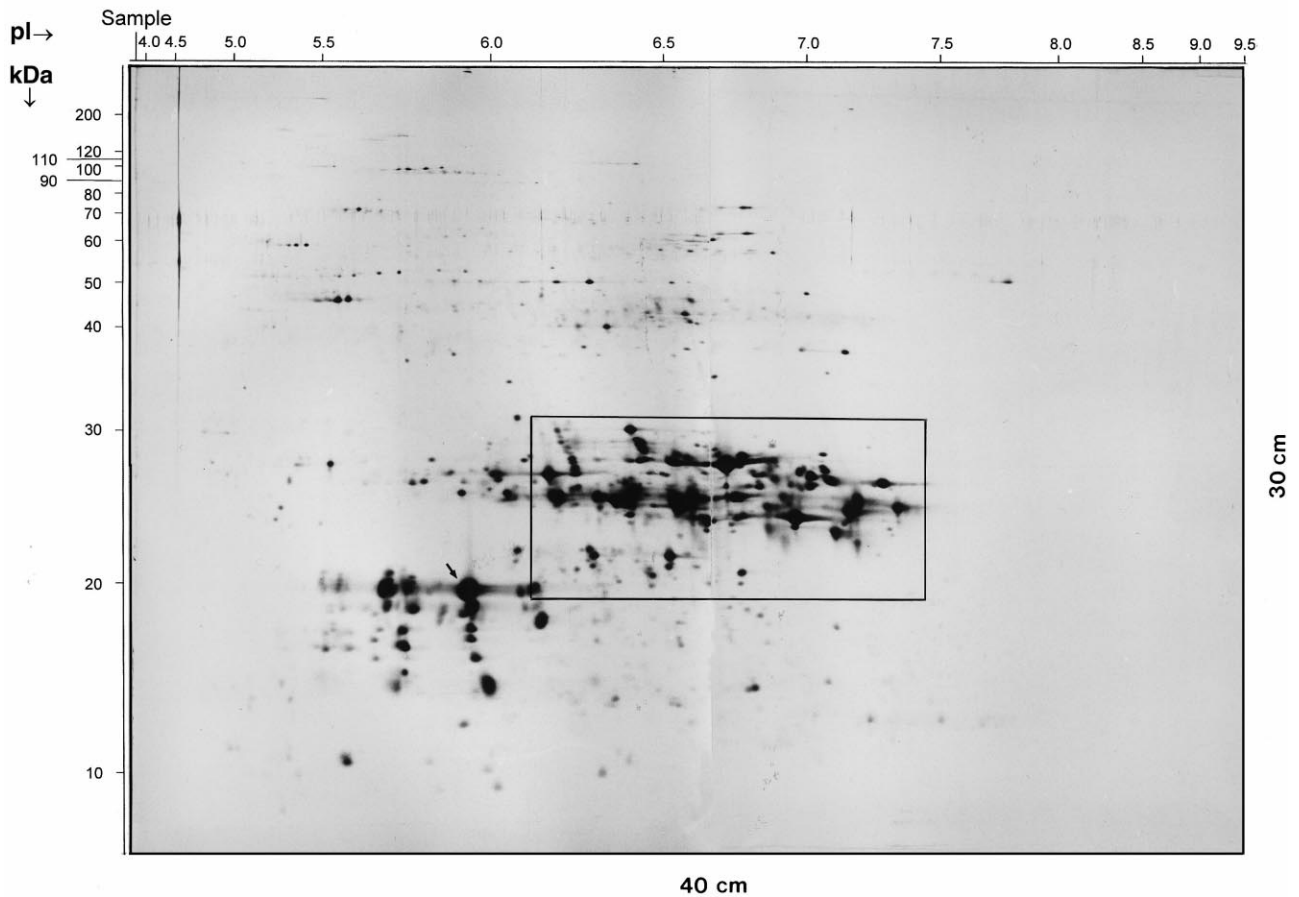


Fig. 1. Total eye lens proteins of the mouse separated by large gel 2D electrophoresis. Indicated section: see Fig. 2. Arrow: Crystallin ( $\alpha$ -A (spot 25 in Table 1).

Manchester, UK). For mass determination by MALDI-MS and post-source decay (PSD) sequencing the mass spectrometer Voyager Elite (PerSeptive, Framingham, MA, USA) with delayed extraction and reflection was employed. A saturated solution of  $\alpha$ -cyano-4-hydroxycinnamic acid in aqueous 50% acetonitrile and 0.1% v/v TFA was used as the matrix. Matrix and sample were mixed on the target (1:1 v/v).

### 3. Results

A 2D electrophoresis pattern of total proteins from a pair of normal mouse eye lenses is shown in Fig. 1. The 10 patterns compared from individual animals for constructing the standard pattern were found to be almost identical with regard to the relative position and intensity of the spots. The high reproducibility may in part result from the fact that the lens itself is a very reproducible organ. It is almost free of foreign tissue, shows reduced metabolic activity and contains well soluble proteins. Patterns from different fractions of lens proteins, i.e. from the water-soluble and urea-soluble fractions [23], did not reveal fraction-specific protein spots or spots not detectable in the total lens extract as used here (results not shown). Furthermore, changes in the protein patterns, which may be due to variations in age (33–51 weeks) or sex, were not observed in the set of mice investigated. The resulting standard pattern of total mouse lens proteins revealed 1940 spots. In the section pH 6.0–7.5/20–24 kDa a number of highly abundant protein spots occurred (Fig. 2), most likely the crystallins. Out of these, 19 spots were selected for partial amino

acid sequencing and peptide mass determination. The data obtained were used to screen the SwissProt, PIR and NCBI GenBank databases for sequence or mass matches.

Peptide mass fingerprinting from on-blot digests by MALDI-MS without delayed extraction was, in most cases, not useful for identifying crystallins down to the level of individual species. Discrimination between highly similar crystallin species was successful only when the distinguishing peptide was sequenced by Edman degradation or PSD-MALDI-MS. Mostly, this afforded sequencing of several peptides to find a discriminative peptide. For example, to elucidate the three protein species ( $\gamma$ -B, D and E, within spot No. 224, 11 peptides had to be sequenced.

The spots identified in the lens protein pattern are shown in Fig. 2 and listed in Table 1. Out of the 16 different crystallins known to occur ubiquitously in mammalian eye lenses, 14 were identified within the 19 analyzed spots by peptide mass fingerprinting, Edman degradation or PSD sequencing. The one missing crystallin, ( $\gamma$ -F, has a high sequence similarity with ( $\gamma$ -E. Mouse ( $\gamma$ -F (NCBI ID g56720) differs from ( $\gamma$ -E (PIR ID JS0596) in five amino acids: G-S, G-A, T-A, S-T, K-R. These exchanges should not result in a pI shift. According to others [29], ( $\gamma$ -F is identical with ( $\gamma$ -E. Interestingly, we found three spots for ( $\gamma$ -E.

Both ( $\gamma$ -B spot 224 and ( $\gamma$ -C spot 239 contained a modified tryptophan at two different positions. In both cases tryptophan was oxidized to kynurenine, which was clearly detectable by a mass shift of +4 in the respective peptide. Spots 223

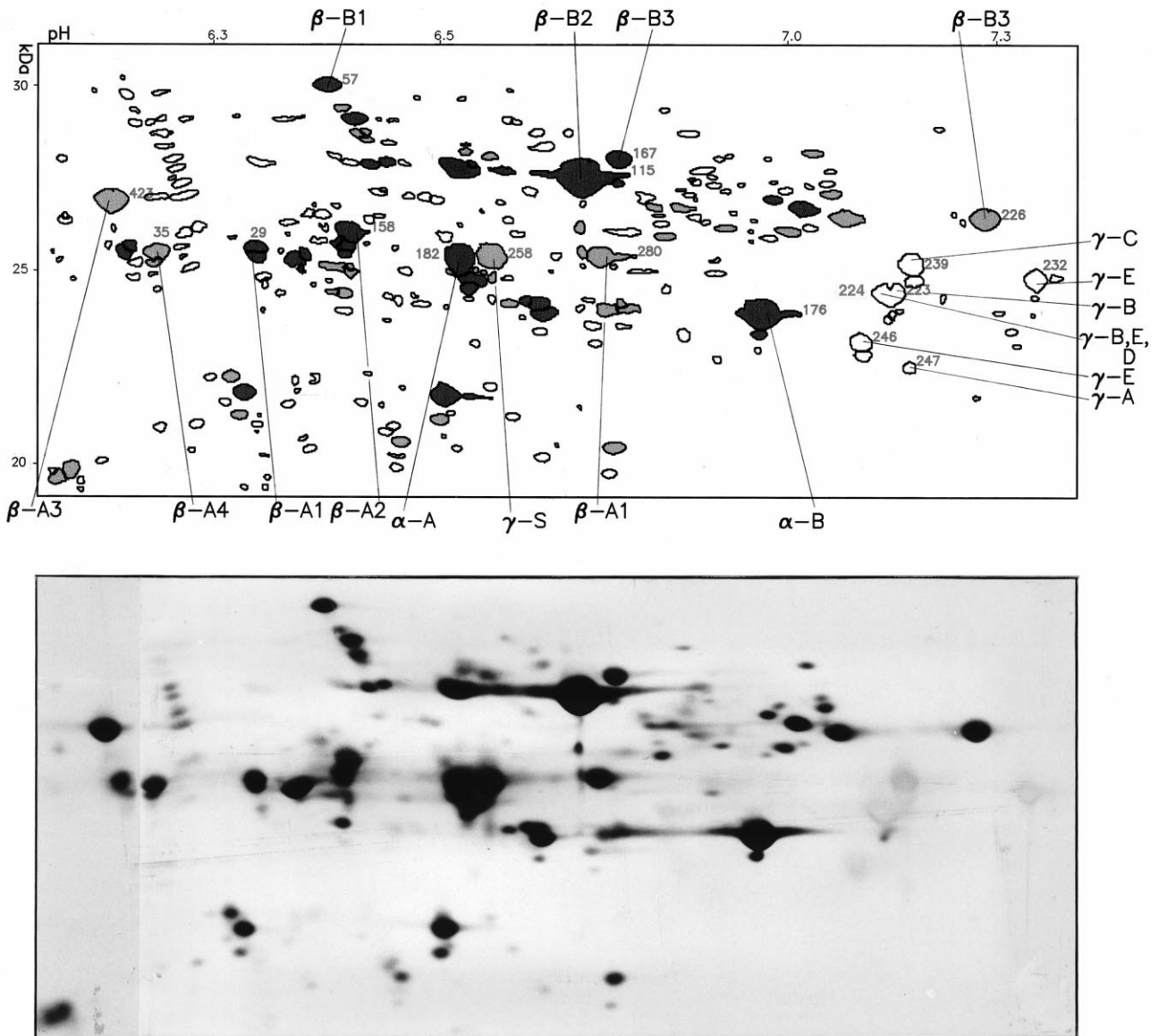


Fig. 2. Section of the mouse eye lens protein pattern shown in Fig. 1 in combination with a computer pattern obtained by image analysis of this section. The protein spots identified so far are indicated. In contrast to the pattern shown in Fig. 1, the proteins were stained just briefly in order to reveal the major spots more distinctly. Consequently, the ( $\gamma$ )-crystallins, which under this conditions stain yellow, occur faintly in the photograph (for full staining see Fig. 3a).

and 224 belong to PIR S33523. Two spots were detected for each of the following crystallins: ( $\alpha$ )-A (No. 182 and arrow in Fig. 1), ( $\beta$ )-A1 (Nos. 29 and 280) and ( $\beta$ )-B3 (Nos. 167 and 226). To identify a protein at the protein species level it is imperative that each peptide determined matches for 100% with the corresponding mouse protein of the sequence database. This was not the case for spot 29, where most of the amino acids matched with ( $\beta$ )-A1 except one amino acid and one peptide containing five amino acids. Apparently, this protein is a subform of ( $\beta$ )-A1 not described in the sequence database. Other non-fitting amino acids occurred in our database search only in assignments of crystallins to different organisms as indicated by bold letters in Table 1. One spot, 224, contained peptides of three crystallins, ( $\gamma$ )-B, D and E. All other protein spots identified revealed only one crystallin species. In two cases differentiation between very similar subspe-

cies was not possible: the single sequence obtained for spot 182 (( $\alpha$ )-A) did not allow us to discriminate between CRAA\_RAT, a protein species common to mouse and rat, and CRA2\_MOUSE, and the sequences detected for ( $\gamma$ )-E were common to three subspecies in the database, CYSMSG2, JS0596, and S26811. Only one spot and without any contamination by other crystallins was detected for ( $\alpha$ )-B, ( $\beta$ )-A2-4, ( $\beta$ )-B1, ( $\beta$ )-B2, ( $\gamma$ )-A and ( $\gamma$ )-S.

For the crystallins ( $\beta$ )-A2-4, ( $\beta$ )-B1 and 3 and ( $\gamma$ )-S sequence data available in databases were from mammalian species other than the mouse. Here, we used the rat for comparison, as far as possible, otherwise human and bovine. Generally, crystallins of the same type differ between these species less than different types of crystallins within a species. For example, the percentages sequence similarity for mouse crystallins ( $\gamma$ )-A, ( $\gamma$ )-E, ( $\gamma$ )-B, ( $\beta$ )-B2, ( $\beta$ )-A1 relative to ( $\gamma$ )-A

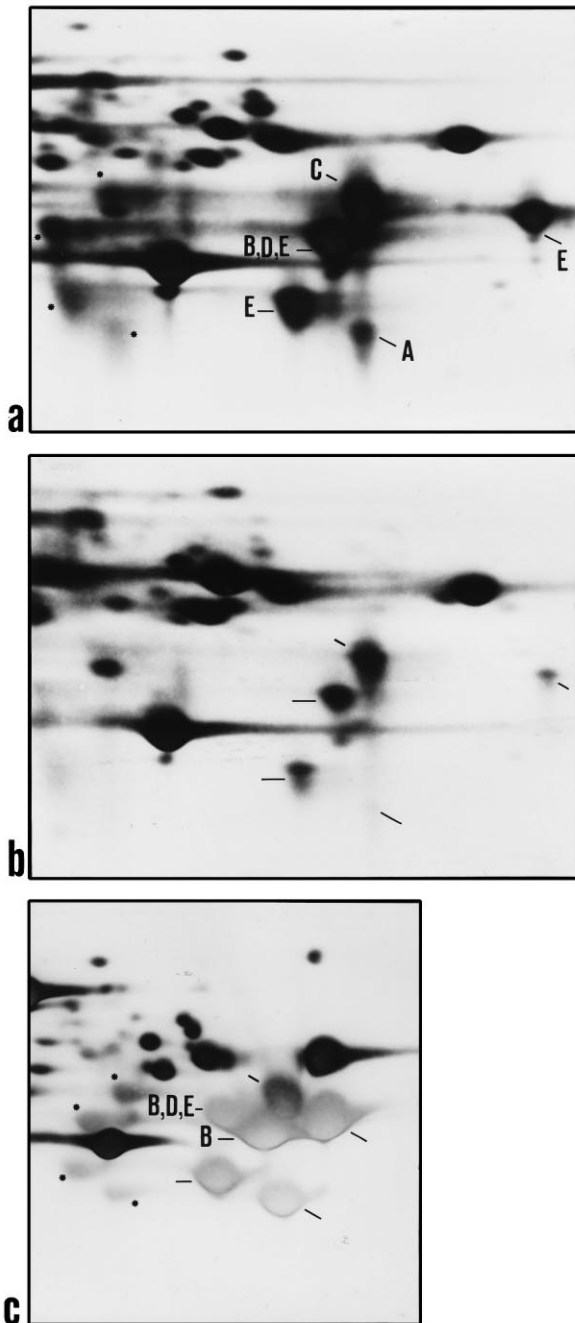


Fig. 3. The  $(\gamma)$ -crystallin region of 2D patterns from mouse lens proteins. a: Normal mouse. The  $(\gamma)$ -crystallins (A, B, D, and E) are fully expressed; a set of minor spots occurs (\*) which reflect the composition and the red-brown color of the  $(\gamma)$ -crystallin spots. b: Mouse cataract mutant *Nop*. The  $(\gamma)$ -crystallin spots are drastically reduced in size and intensity,  $(\gamma)$ -A and the set of minor spots (see \* in panel a) disappeared completely. Note that other spots also show quantitative changes compared to the normal pattern. c: Normal mouse. The proteins were run under different conditions (altered composition of the ampholyte mixture, brief staining) for better separation of  $(\gamma)$ -B from  $(\gamma)$ -D/E crystallins.

(CRGA\_MOUSE) were 100%, 79.4%, 60.8%, 32.1%, 24.6%, respectively. The percentages sequence similarity of mouse against rat, human and bovine for  $(\gamma)$ -A (CRGA\_MOUSE) were 97.3%, 85.4%, 69.5%, respectively. The amino acid sequences of rat, human and bovine  $(\beta)$ -A4, as another exam-

ple, share 92–94% sequence similarity [16] and therefore, all three mammalian species were helpful in identifying  $(\beta)$ -A4 in the mouse. We identified most of the crystallins on the basis of specific sequences (Table 1).

Considering the position of the identified protein spots in the 2D pattern (Fig. 2) it is obvious that the various  $(\gamma)$ -crystallins are situated closely together in one region, except for  $(\gamma)$ -S. The  $(\gamma)$ -D/E spot overlaps largely with one  $(\gamma)$ -B spot (Fig. 3a). However, when using our ampholyte standard mixture [21], these overlapping spots split into two spots (Fig. 3c) and were blotted under these conditions for sequencing. The  $(\gamma)$ -crystallin spots (except  $(\gamma)$ -S) were distinct from all other spots by developing a yellow color in our silver staining procedure [21]. A few other yellow spots were observed in this region apparently representing a set of minor spots split from the major set of  $(\gamma)$ -crystallins (Fig. 3a,c). The  $(\beta)$ -A crystallins and the  $(\beta)$ -B crystallins also form groups of spots in our 2D pattern (Fig. 2), but very loosely.

In protein patterns of the cataract mutant *Nop* the intensity (amount) of the whole  $(\gamma)$ -crystallin spot complex, with the exception of  $(\gamma)$ -S, was drastically reduced (Fig. 3).  $(\gamma)$ -E (the most basic spot in Fig. 3a), rather than the mutant  $(\gamma)$ -B crystallin, was preferentially reduced. Quantitative changes, i.e. decreased or increased intensities, were also observed for a number of other spots, including crystallin spots, but the reduction of the  $(\gamma)$ -crystallin spots was the most striking finding made in the lens protein patterns of these mouse mutants. Preliminary results from an investigation of six other mouse cataract mutants also showed quantitative changes for many spots of the lens protein pattern. These changes were reproducible and, on the whole, characteristic for each cataract mutant line.

#### 4. Discussion

In this investigation we presented a 2D electrophoresis pattern of total mouse eye lens proteins revealed under conditions for maximum resolution. By densitometry and computer-assisted image analysis 1940 protein spots were detected. By protein sequencing and mass spectrometry all 16 crystallins ubiquitous in mammals were identified as separate spots, with the exception of  $(\gamma)$ -F, which shows an identical or an almost identical sequence to  $(\gamma)$ -E;  $(\gamma)$ -D was mixed with B and E. Two crystallins,  $(\beta)$ -A2 and  $(\gamma)$ -S, were shown for the first time to occur in the mouse lens,  $(\beta)$ -A2,  $(\beta)$ -B1 and 3, and  $(\gamma)$ -A, B, D, E were demonstrated for the first time in an electrophoretic 2D pattern.

Identification of protein species within a protein family affords more sequence information than assignment of a protein spot to a protein family, which has been the identification aim for the annotation of most of the 2D protein databases collected in the federated world 2D protein database (URL: <http://expasy.hcuge.ch/ch2d/2d-index.html>) [30]. Here we have shown the successful identification and discrimination of all known members of a protein family revealed in a 2D gel.

The spontaneous dominant cataract mutant *Nop* of the mouse was detected by Graw et al. [9] and described as nuclear opacity of the lens. Recently the *Nop* mutation was found in the  $(\gamma)$ -B crystallin gene [9]. Isoelectric focusing of water-soluble lens proteins from *Nop* mice showed a reduced content of  $(\gamma)$ -crystallin [10,11], a finding supported by North-

ern blot results [12]. The ( $\gamma$ )-crystallins, however, result from six individual genes organized as a cluster. Although only one gene was affected in the *Nop* mutant, our 2D analysis of the *Nop* lens proteins showed that each of the six ( $\gamma$ )-crystallins was heavily reduced in quantity, ( $\gamma$ )-E (the most basic spot) more than the other ones; ( $\gamma$ )-S, a more distantly related ( $\gamma$ )-crystallin, was not altered. In the heterozygote protein pattern (Fig. 3b), the ( $\gamma$ )-B isoforms detected in the wild-type pattern were present, but a candidate spot for the *Cat2<sup>nop</sup>* allele, i.e. for a ( $\gamma$ )-B crystallin truncated by the loss of 32 amino acids [9], was not observed. Quantitative changes in protein spots other than those identified as ( $\gamma$ )-crystallins were found.

The analysis of the mouse *Nop* mutation by 2D electrophoresis demonstrated that monogenic mutations may have pleiotropic effects involving a broad spectrum of proteins. Histological investigations of *Nop* lenses have shown that lens fiber cell differentiation was impaired (impaired elongation of the fiber cells, prolonged presence of fiber cell nuclei) [9]. This may suggest that the pleiotropic effect was a consequence of morphological alterations of the lens. However, *Nop* lenses studied during embryonic development revealed as the first alteration, preceding morphological changes, a reduced level of ( $\gamma$ )-crystallin mRNA [31]. Studies on early stages of normal and mutant lenses on the basis of highly resolved 2D protein patterns might allow us to follow the single steps of pathogenesis leading to cataract phenotypes. For this purpose, however, more proteins need to be identified in 2D patterns of the eye lens.

## References

- [1] Wistow, G. (1995) *Molecular Biology and Evolution of Crystallins: Gene Recruitment and Multifunctional Proteins in the Eye Lens*, Springer Verlag, New York.
- [2] Delaye, M. and Tardieu, A. (1983) *Nature* 302, 415–417.
- [3] Favor, J. (1984) *Genet. Res. Camb.* 44, 183–197.
- [4] Kratochvilova, J. and Favor, J. (1988) *Genet. Res. Camb.* 52, 125–134.
- [5] Kratochvilova, J. and Favor, J. (1992) *Genet. Res. Camb.* 59, 199–203.
- [6] Favor, J. and Pretsch, W. (1990) *Genet. Res. Camb.* 56, 157–162.
- [7] Everett, C.A., Glenister, P.H., Taylor, D.M., Lyon, M.F., Kratochvilova-Loester, J. and Favor, J. (1994) *Genomics* 20, 429–434.
- [8] Löster, J., Pretsch, W., Sandulache, R., Schmitt-John, T., Lyon, M.F. and Graw, J. (1994) *Genomics* 23, 240–242.
- [9] Klopp, N., Favor, J., Löster, J., Lutz, R.B., Neuhäuser-Klaus, A., Prescott, A., Pretsch, W., Quinlan, R.A., Sandilands, A., Vrensen, G.F.J.M. and Graw, J. (1998) *Genomics* (in press).
- [10] Graw, J., Kratochvilova, J. and Summer, K.-H. (1984) *Exp. Eye Res.* 39, 37–45.
- [11] Doria, R., Graw, J. and Maier, K. (1984) *Curr. Eye Res.* 3, 723–728.
- [12] Graw, J., Werner, T., Merkle, S., Reitmeir, P., Schaffer, E. and Wulff, A. (1990) *Exp. Eye Res.* 50, 449–456.
- [13] Ringens, P.J., Hoenders, H.J. and Bloemendal, H. (1982) *Exp. Eye Res.* 34, 815–823.
- [14] Datiles, M.B., Schumer, D.J., Zigler Jr., J.S., Russel, P., Anderson, L. and Garland, D. (1992) *Curr. Eye Res.* 11, 669–677.
- [15] Garland, D.J., Douglas-Tabor, Y., Jimenez-Asensio, J., Datiles, M.B. and Magno, B. (1996) *Exp. Eye Res.* 62, 285–291.
- [16] Bloemendal, H., Van de Gaer, K., Benedetti, E.L., Dunia, I. and Steely, H.T. (1997) *Ophthalmic Res.* 29, 177–190.
- [17] Lampi, K.J., Ma, Z., Shih, M., Shearer, T.R., Smith, J.B., Smith, D.L. and David, L.L. (1997) *J. Biol. Chem.* 272, 2268–2275.
- [18] Garber, A.T., Stirk, L. and Gold, R.J. (1983) *Exp. Eye Res.* 36, 165–169.
- [19] Calvin, H.I., Wu, J.X., Viswanadhan, K. and Fu, S.C.J. (1996) *Exp. Eye Res.* 63, 357–368.
- [20] Tumminia, S.J., Jonak, G.J., Focht, R.J., Cheng, Y.S.E. and Russell, P. (1996) *J. Biol. Chem.* 271, 425–431.
- [21] Klose, J. and Kobalz, U. (1995) *Electrophoresis* 16, 1034–1059.
- [22] Ehling, U.H. (1991) *Annu. Rev. Genet.* 25, 255–280.
- [23] Klose, J. (1998) in: *Methods in Molecular Biology* (Altria, K., Ed.) 2-D Protocols for Proteome Analysis (Link, A.J. Ed.), Chapter 9, Humana Press, Totowa, NJ (in press).
- [24] Klose, J. (1998) in: *Methods in Molecular Biology* (Altria, K., Ed.) 2-D Protocols for Proteome Analysis (Link, A.J. Ed.), Chapter 18, Humana Press, Totowa, NJ (in press).
- [25] Prehm, J., Jungblut, P. and Klose, J. (1987) *Electrophoresis* 8, 562–572.
- [26] Jungblut, P., Eckerskorn, C., Lottspeich, F. and Klose, J. (1990) *Electrophoresis* 11, 581–588.
- [27] Otto, A., Thiede, B., Müller, E.-C., Scheler, C., Wittmann-Liebold, B. and Jungblut, P. (1996) *Electrophoresis* 17, 1643–1650.
- [28] Thiede, B., Otto, A., Zimny-Arndt, U., Müller, E.C. and Jungblut, P. (1996) *Electrophoresis* 17, 588–599.
- [29] Graw, J. (1996) *Dev. Genet.* 18, 181–197.
- [30] Appel, R.D., Bairoch, A., Sanchez, J.-C., Vargas, J.R., Golaz, O., Pasquali, C. and Hochstrasser, D.F. (1996) *Electrophoresis* 17, 540–546.
- [31] Santhiya, S.T., Moustafa Abd-alla, S., Löster, J. and Graw, J. (1995) *Graefes Arch. Clin. Exp. Ophthalmol.* 233, 795–800.